Spontaneous Core Rotation in Ferrofluid Pipe Flow

Alexei Krekhov[1] and Mark Shliomis[2]

[1]*Max Planck Institute for Dynamics and Self-Organization, 37077 Göttingen, Germany*
[2]*Department of Mechanical Engineering, Ben-Gurion University of the Negev, Beer-Sheva 84105, Israel*

Ferrofluid flow along a tube of radius R in a constant axial magnetic field is revisited. Our analytical solution and numerical simulations predict a transition from an initially axial flow to a steady swirling one. The swirl dynamo arises above some critical pressure drop and magnetic field strength. The new flow pattern consists of two phases of different symmetry: The flow in the core resembles Poiseuille flow in a rotating tube of the radius $r_* < R$, where each fluid element moves along a screw path, and the annular layer of the thickness $R - r_*$, where the flow remains purely axial. These phases are separated by a thin domain wall. The swirl appearance is accompanied with a sharp increase in the flow rate that might serve for the detection of the swirling instability.

Rotating flows arising in the absence of obvious sources of rotation are rather widespread. Swirl generation is observed in spiral galaxies, hurricanes, tornadoes, or dust devils. An everyday manifestation of the phenomenon is the vortex in the drain of a bathtub or a kitchen sink. Earlier studies supposed [1] that the vortex is driven by Coriolis forces, which are counterclockwise in the Northern hemisphere of Earth and clockwise in the Southern one, and this assertion was confirmed both in Boston, Massachusetts [1] and Sydney, Australia [2]. Later, however, careful experiments [3,4] have shown that the rotation occurs in consequence of a supercritical bifurcation as the speed of swirl-free sink flow exceeds some threshold value, while Earth's rotation only removes the twofold degeneracy of the swirl direction, making the bifurcation a tiny bit imperfect [5].

One amazing example of self-rotation was discovered 120 years ago by Quincke [6]. He reported that dielectric spheres and cylinders suspended in weakly conducting liquids would spin spontaneously when subjected to strong enough electrostatic fields. To explain this effect [7], modern theory [8,9] uses the concept of an effective dipole directed against the applied field. Since this orientation is unstable, the sample starts to spin if the electric torque overcomes the viscous one.

Spontaneous rotation of insulating liquids inside electrified menisci was studied in great detail. Above some critical voltage, the meniscus acquires a shape referred to as the Taylor cone [10], and the fluid is injected through its apex [11]. Self-rotation caused by the electric stress acting on the gas-liquid interface appears as bifurcation from a primary swirl-free meridional flow [12,13].

Here we present a novel, very unusual, swirl dynamo arising in an originally axial pipe flow of a ferrofluid under the action of a constant longitudinal magnetic field. This Hagen-Poiseuille flow in both constant and oscillating magnetic fields has been widely studied experimentally [14–20] and theoretically [17,20–25]. At small shear rates, $\Omega\tau \ll 1$ (2Ω is

the flow vorticity, τ stands for the magnetization relaxation time), the velocity profile remains parabolic, but the flow rate is reduced due to the increase of viscosity (the so-called *magnetoviscous effect* [21,26]). With larger pressure drops ($\Omega\tau > 1$), the magnetoviscosity becomes dependent on the shear rate as well [21,24,26–29]—the ferrofluid acquires non-Newtonian properties. Since the shear rate in pipe flow is nonuniform over the pipe cross section, magnetoviscosity is obviously a function of radial distance r; hence, the flow profile ceases to be parabolic.

In the previous investigations, the ferrofluid pipe flow was always assumed to be purely axial. We remove this restriction and demonstrate that the specific dependence of magnetoviscosity on the shear rate leads to swirling instability. The term "swirl" denotes here screw streamlines in the core and straight ones near the wall. With the appearance of azimuthal component of the velocity, its axial component increases. The latter may be treated as a manifestation of the Le Chatelier principle: the magnetic field reduces the flow rate because of magnetoviscosity but gives rise to swirl, which counteracts the magnetoviscous effect and thus maintains the flow rate.

Basic equations.—The conventional set of hydrodynamic equations for incompressible ferrofluids [21,30] consists of the generalized Navier-Stokes equation (1), the magnetization equation (2), and Maxwell's magnetostatic equations (3):

$$\rho \frac{d\mathbf{v}}{dt} = -\nabla p + \eta \nabla^2 \mathbf{v} + (\mathbf{M} \cdot \nabla)\mathbf{H} + \frac{1}{2}\nabla \times (\mathbf{M} \times \mathbf{H}),$$

$$(1)$$

$$\frac{d\mathbf{M}}{dt} = \mathbf{\Omega} \times \mathbf{M} - \frac{1}{\tau}(\mathbf{M} - \chi\mathcal{L}\mathbf{H})$$

$$-\frac{3\chi(1-\mathcal{L})}{2\tau M^2}\mathbf{M} \times (\mathbf{M} \times \mathbf{H}), \quad (2)$$

$$\nabla \times \mathbf{H} = 0, \qquad \nabla \cdot (\mathbf{H} + 4\pi\mathbf{M}) = 0. \tag{3}$$

Here, $d/dt = \partial/\partial t + (\mathbf{v} \cdot \nabla)$, $\mathbf{M}$ stands for the ferrofluid magnetization, $\mathcal{L} = 3L(\zeta)/\zeta$, where $L(\zeta) = \coth\zeta - 1/\zeta$ is the Langevin function, $\boldsymbol{\Omega} = \frac{1}{2}\nabla \times \mathbf{v}$, p is the pressure, ρ and η are the ferrofluid density and viscosity, χ is the initial magnetic susceptibility.

In the true equilibrium ($\mathbf{v} = 0$, $\mathbf{H} = \text{const}$) the solution of Eq. (2) is described by the expression $\mathbf{M}_{\text{eq}} = (M_s/3)\mathcal{L}(\xi)\boldsymbol{\xi}$, where $\boldsymbol{\xi} = 3\chi\mathbf{H}/M_s$ represents the nondimensional magnetic field, and $M_s = \phi M_b$ is the saturation magnetization (ϕ is the volume fraction of dispersed ferromagnetic grains, M_b is their bulk magnetization). Out of equilibrium, $\mathbf{M}$ and $\mathbf{H}$ are independent variables: $\mathbf{M}$ may exist (as typically transient) even in the absence of $\mathbf{H}$. It is convenient, nonetheless, to consider any instantaneous magnetization as an equilibrium one in a certain nondimensional "effective" field $\boldsymbol{\zeta}$: $\mathbf{M} = (M_s/3)\mathcal{L}(\zeta)\boldsymbol{\zeta}$. In equilibrium, of course, $\boldsymbol{\zeta} = \boldsymbol{\xi}$.

The range of validity of Eqs. (1), (2) is limited to the weakly nonideal (WNI) ferrofluids (in the model of ideal ones, interaction between magnetic grains is assumed to be negligible). Most of the commercial ferrofluids belong to the WNI type: interparticle interactions are able to magnify essentially the initial magnetic susceptibility χ, but do not provide the chainlike particle associations. As shown in Ref. [31], dipolar particles form short chains and small rings when the dimensionless coupling parameter λ (the ratio of the energy of two adjoining grains to the thermal energy) is more than 2 [32], while in commercial ferrofluids there is typically $\lambda < 1$. Allowance for the magnetic interactions in WNI ferrofluids can be realized by the replacement of the Langevin's magnetic susceptibility $\chi_L = mM_s/(3k_BT)$ of ideal ferrofluid (here m is the particle magnetic moment) by $\chi = \chi_L(1 + 4\pi\chi_L/3)$ in the Langevin parameter ξ, that yields a quite good approximation for many ferrofluids [33].

Analytical solution.—Let us start with Eqs. (1)–(3) written in the dimensionless form—see Ref. [34]—using as unit of length R, time τ, velocity R/τ, pressure η/τ, magnetic field $M_s/(3\chi)$, and the magnetization $M_s/3$. In cylindrical coordinates (r, φ, z) with the axis z along the pipe axis, the above-mentioned vectors have components $\mathbf{v} = (0, v_\varphi, v_z)$, $\boldsymbol{\Omega} = (0, \Omega, \omega)$, $\boldsymbol{\zeta} = (\zeta_r, \zeta_\varphi, \zeta_z)$, and $\boldsymbol{\xi} = (\xi_r, 0, \xi_0)$. All these quantities (apart from ξ_0 that represents the uniform applied field H_0) depend on r and t. The regular solution of the second of Eqs. (3) is given by $\xi_r = -(\mu - 1)\mathcal{L}\zeta_r$, where $\mu = 1 + 4\pi\chi$ is the initial magnetic permeability.

In the case of low to moderate magnetization, when $\mathcal{L}(\zeta) = 1 - \zeta^2/15 + O(\zeta^4)$, one can replace everywhere $\mathcal{L}$ with unity. Then, for a steady flow, one finds from Eq. (2)

$$\zeta_r = \frac{\xi_0\Omega}{\Omega^2 + \Lambda^2 + \mu}, \qquad \zeta_\varphi = \Lambda\zeta_r, \qquad \zeta_z = \frac{\Lambda^2 + \mu}{\Omega}\zeta_r,$$

$$\tag{4}$$

where $\Omega = -(dv_z/dr)/2$. Furthermore, instead of the axial component of the angular velocity $\omega = (2r)^{-1}d(rv_\varphi)/dr$, we have introduced a new variable,

$$\Lambda = \omega - \frac{v_\varphi}{r} = \frac{1}{2}\left(\frac{dv_\varphi}{dr} - \frac{v_\varphi}{r}\right) = \frac{r}{2}\frac{d}{dr}\left(\frac{v_\varphi}{r}\right). \tag{5}$$

As seen from the definition, $\Lambda = 0$ either in the absence of fluid rotation $v_\varphi = 0$, or if the liquid concentric cylinder of radius r rotates with a uniform angular velocity $v_\varphi/r = \text{const}$. Nonzero $\Lambda(r)$ arises only when different annular liquid layers rotate differently.

After integration of azimuthal and axial steady-state components of Eq. (1) [36] with boundary conditions $v_\varphi = v_z = 0$ at $r = 1$, and elimination of $\boldsymbol{\zeta}$ components [using Eqs. (4) and the relation $\xi_r = -(\mu - 1)\zeta_r$], we obtain

$$\Lambda\left(1 - \frac{h^2\Omega^2}{(\Omega^2 + \Lambda^2 + \mu)^2}\right) = 0, \tag{6}$$

$$\Omega\left(1 + \frac{h^2(\Omega^2 + \mu\Lambda^2 + \mu^2)}{(\mu - 1)(\Omega^2 + \Lambda^2 + \mu)^2}\right) = Pr. \tag{7}$$

Here we introduced two dimensionless parameters, h and P. The former is linked with ξ_0 and H_0 by the simple relations, the latter stands for the pressure gradient:

$$h = \xi_0\frac{M_s}{3}\sqrt{\frac{\pi\tau}{\eta}} = \chi H_0\sqrt{\frac{\pi\tau}{\eta}}, \qquad P = \frac{\tau R}{4\eta}\left(\frac{\Delta p}{l}\right),$$

where Δp is the pressure drop over the pipe length l.

Instability of the axial flow.—In the presence of rotation ($\Lambda \neq 0$), Eq. (6) is satisfied with the equality

$$h\Omega = \Omega^2 + \Lambda^2 + \mu, \tag{8}$$

which determines Λ as a function of Ω:

$$\Lambda^2 = (\Omega - \Omega_1)(\Omega_2 - \Omega), \qquad \Omega_{1,2} = \frac{1}{2}\left(h \mp \sqrt{h^2 - 4\mu}\right). \tag{9}$$

Note that the sign of Λ (and, consequently, the direction of fluid rotation) remains uncertain. Now Eq. (8) allows us to eliminate Λ^2 from Eq. (7):

$$\frac{\mu h}{\mu - 1} = Pr. \tag{10}$$

Thus, Λ differs from zero only on the cylindrical surface of the radius $r_* = \mu h/[(\mu - 1)P]$. As we demonstrate below, this result—Λ is the δ function of $(r - r_*)$—is a consequence of the linear approximation in ζ: even a weak nonlinearity of the magnetization law turns $\Lambda(r)$ into a smooth function. Meantime, $\Lambda(\Omega)$ takes on the surface

(a)

(b)
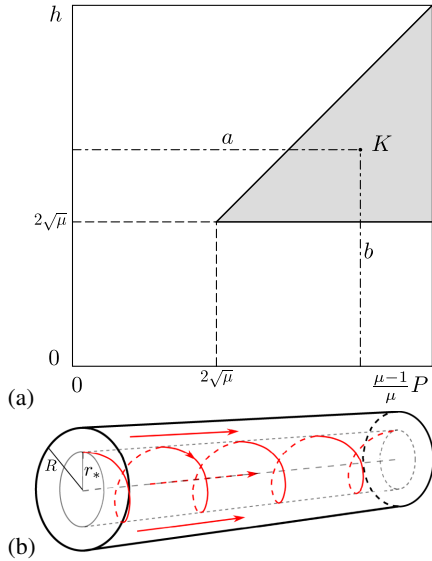
FIG. 1.   Stability diagram in the $P - h$ plane (a). In the region of swirling flow (shaded) coordinates of any point K determine the radius $r_* = b/a$ of a rotating liquid cylinder. Sketch of the swirling flow (b).

$r = r_*$ entire values between 0 at $\Omega = \Omega_{1,2}$ and its maximum $\Lambda_{\mathrm{m}} = \sqrt{h^2/4 - \mu}$ at $(\Omega_1 + \Omega_2)/2 = h/2$.

The dimensionless effective viscosity η_{eff} is given by the expression in large parentheses of Eq. (7). Hence, rewriting Eq. (10) in the form

$$\Omega\left(\frac{\mu h}{(\mu - 1)\Omega}\right) = Pr,$$

we find the viscosity jump with respect to the two sides of the surface of *discontinuity*:

$$[\eta_{\mathrm{eff}}]_{r_*+0}^{r_*-0} = \frac{\mu h}{\mu - 1}\left(\frac{1}{\Omega_1} - \frac{1}{\Omega_2}\right) = \frac{2h\Lambda_m}{\mu - 1}. \quad (11)$$

Insofar as viscosity decreases with increasing shear rate, the fluid is most viscous in the core [37].

Swirling flow occurs at $h > h_c = 2\sqrt{\mu}$ (when $\Omega_1 = \Omega_2 = \sqrt{\mu}$) and $P > \mu h/(\mu - 1)$. When these conditions are met, one has $r_* < 1$. The region of swirling flow is limited by two straight boundary lines: $h = (\mu - 1)P/\mu$ from the left and $h = h_c$ from below—see Fig. 1(a). The flow pattern is formed out of a liquid cylinder of radius r_* and an annular layer of thickness $1 - r_*$. The core rotates with a constant angular velocity $\Theta = v_\varphi/r$ in addition to the axial flow $v_z(r)$; thus, any of its elements moves along a corkscrew trajectory of the radius r and with the pitch $2\pi v_z(r)/\Theta$. Meantime, streamlines of the fluid occupying the annular layer are left to be straight [see Fig. 1(b)].

Numerical results.—To test the validity range of analytical results obtained for small to moderate magnetization, we have performed direct numerical simulations of
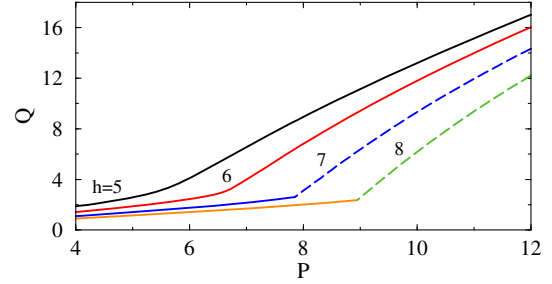
FIG. 2.   Volume flow rate Q as a function of the pressure gradient P for ferrofluid with $\mu = 9$ at different values of magnetic field h. Solid lines—purely axial flow, dashed lines —swirling flow.

Eqs. (1)–(3) (see Ref. [24] for details of the numerical method). The strong variations in the velocity and magnetization components near r_* have been resolved using spatial discretization steps down to 10^{-4}.

For steady flows, solutions of Eqs. (1)–(3) depend on two dimensionless material parameters, μ and $E = M_s^2\tau/(18\eta\chi)$, and two control parameters, P and ξ_0. Equally, with the latter we use the field parameter h linked with ξ_0 by the relation $h = \xi_0\sqrt{(\mu - 1)E/2}$. The three different pairs of μ-E values we used [34] cover a wide range of real ferrofluids.

Our numerical stability analysis indeed confirms that the axial steady flow becomes unstable inside the shaded region in Fig. 1(a). The stability boundaries found numerically for three different sets of the material parameters agree within an accuracy of $(1 - 3)\%$ with analytical results obtained in the linear approximation in ζ. To explain such a perfect agreement, note that the critical values of effective field ζ_c proved to be close to 0.5 for all three mentioned ferrofluids. For $\zeta = 0.5$, the function $\mathcal{L}(\zeta)$ takes the value 0.984 that differs from its linear approximation, $\mathcal{L}(0) = 1$, by less than 2%.

Simulations of the full nonlinear equations demonstrate that the swirling instability is supercritical.

The onset of the swirling flow is clearly visible in Fig. 2 where the pressure dependence of the volume flow rate $Q = 2\pi\int_0^1 v_z r\,dr$ is presented. Two upper smooth curves correspond to subcritical values of magnetic field $h \leq h_c$ when the flow is purely axial. Each of the two supercritical lower curves consists of parts corresponding to axial (at smaller P) and swirling flows (at larger P) with a kink at the critical point. The swirl appearance leads to a strong increase of the axial velocity (compare the solid and the dashed lines in Fig. 3), that results in a growth of the flow rate. The abrupt increase of Q might serve as a detector of swirling instability in experiments.

Figure 3 shows that the appearance of an azimuthal component of the fluid velocity $v_\varphi(r)$ at $r \leq r_*$ is accompanied with a kink in the graph of the axial velocity $v_z(r)$ at r_*. If, however, the azimuthal component of velocity is
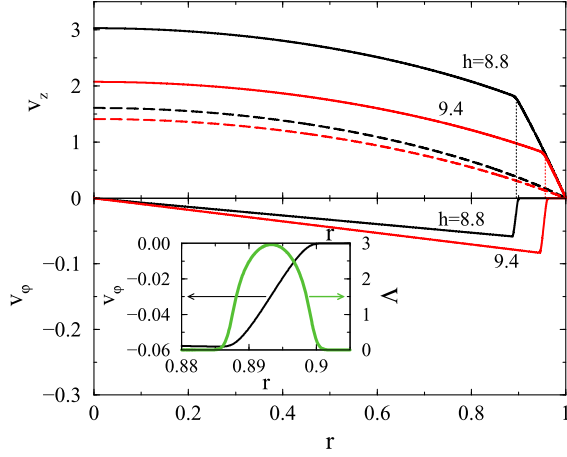
FIG. 3.   Axial, $v_z(r)$, and azimuthal, $v_\varphi(r)$, components of the velocity for ferrofluid with $\mu = 9$ at $P = 11$ and two values of magnetic field h are solid lines. Profiles $v_z(r)$ obtained when the azimuthal component of the velocity is suppressed ($v_\varphi = 0$) are dashed lines. Inset: Enlarged view of $v_\varphi(r)$ and function $\Lambda(r)$ for $h = 8.8$ in the vicinity of $r_* = 0.8931$. The width of $\Lambda(r)$ is $\Delta r = 0.0138$; its maximum magnitude $\Lambda_{\max} = 2.940$.

suppressed in the simulations ($v_\varphi = 0$), the axial velocity $v_z(r)$ remains a smooth function (dashed lines in Fig. 3). The inset in the figure demonstrates an important difference between the results obtained analytically under the assumption of the linear magnetization law, and numerically, keeping safe the nonlinearity of $\mathcal{L}(\zeta)$. In the latter case, Λ ceases to be the δ function of $(r - r_*)$. Even a small deviation of $\mathcal{L}(\zeta)$ from unity is enough to eliminate the tangential discontinuities at r_*. Nonlinearity of the magnetization law "washes away" the domain wall between the uniformly rotating core and the nonrotating surroundings, turning it into a thin *transitional layer* of thickness Δr.

In Fig. 4 components of the dimensionless magnetization $\tilde{\mathbf{M}} = \mathcal{L}(\zeta)\boldsymbol{\zeta}$ are shown for $h = 8.8$ and the same other parameters as in Fig. 3. If the azimuthal component of the velocity is suppressed ($v_\varphi = \Lambda = 0$), solid lines of $\tilde{M}_r$ and $\tilde{M}_z$ change smoothly into dashed lines at r_*, while $\tilde{M}_\varphi$ does not occur at all. It arises simultaneously with Λ at the swirl appearance; indeed, $\tilde{M}_\varphi \propto \zeta_\varphi = \Lambda \zeta_r$ as it is seen from Eq. (4).

Discussion.—The mechanism of swirl generation can be explained within the concept of *internal rotation* [21]. In the absence of a magnetic field, each particle in the ferrofluid pipe flow rolls down the pipe with an angular speed $\Omega(r)$ over the cylindrical shear surface of the radius r. An applied axial field $\mathbf{H}_0$ tends to line up magnetic moments of all magnetic particles parallel to itself and thus impedes free particle rotation: The field turns on the mechanism of magnetoviscosity. Under the action of magnetic and viscous torques upon the particles, the magnetization $\mathbf{M}$ deviates from the field direction: there occurs a radial component of the magnetization together
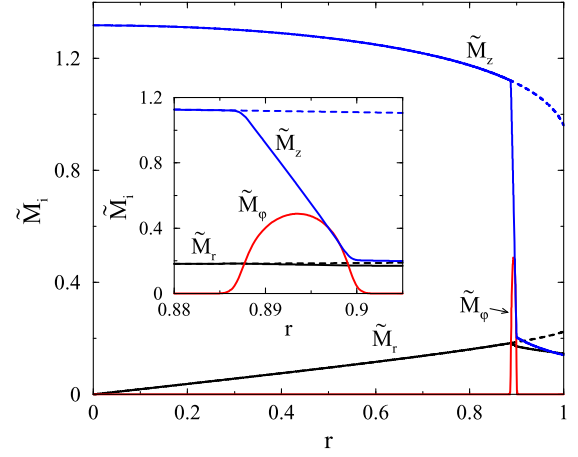
FIG. 4.   Magnetization components $\tilde{M}_i(r)$ for ferrofluid with $\mu = 9$ at $P = 11$ and $h = 8.8$ shown by solid lines. Dashed lines of $\tilde{M}_r(r)$ and $\tilde{M}_z(r)$ continue when the azimuthal component of the velocity is suppressed ($v_\varphi = 0$); in this case $\tilde{M}_\varphi = 0$. Inset: Enlarged view in the vicinity of $r_* = 0.8931$.

with oppositely directed field component $H_r = -4\pi M_r$. The last factor (opposite signs) provides *positive feedback* for the instability of the initially axial ferrofluid pipe flow.

Consider a weak disturbance of the pipe flow: A liquid cylinder of radius r_* turns around clockwise; i.e., its angular velocity is negative. The rotating cylinder spins particles surrounding its surface counterclockwise, such that the vector $\mathbf{M}$ moves out of the $r - z$ plane producing a positive azimuthal component M_φ (see Fig. 4). Just the latter causes the rotation of the liquid cylinder.

Let us calculate the magnetic torque. Its dimensionless specific value (in units of η/τ) is given by the expression

$$\mathfrak{m} = (\mathbf{M} \times \mathbf{H})_z = -2E\xi_r\zeta_\varphi = 4\Lambda, \qquad (12)$$

simplified with the help of Eqs. (4), (8). The total magnetic torque $\mathfrak{M}$ acting on the unit length of the liquid cylinder is found by multiplying the specific torque $\mathfrak{m}$ by $2\pi r$ and integrating over the thickness $\Delta r = 2\varepsilon$ of the transitional layer, within which $\Lambda(r)$ differs from zero:

$$\mathfrak{M} = 8\pi \int_{r_*-\varepsilon}^{r_*+\varepsilon} r\Lambda dr \simeq 4\pi r_*^2 \left[\frac{v_\varphi}{r}\right]_{r_*-\varepsilon}^{r_*+\varepsilon} = -4\pi r_*^2\Theta; \qquad (13)$$

here we took into account the narrowness of the layer ($\varepsilon \ll 1$) and boundary conditions at its inner and outer surfaces, $v_\varphi(r_* - \varepsilon) = v_\varphi^m$, $v_\varphi(r_* + \varepsilon) = 0$, where v_φ^m means the maximum (minimum) azimuthal velocity.

Thus, the appearance of a positive M_φ gives rise also to a positive magnetic torque $\mathfrak{M}$ (having opposite sign of the rotational speed $\Theta = v_\varphi^m/r_*$), which intensifies the particle rotation and accelerates it by the initial clockwise rotation of the core. The torque (13) is balanced by the moment of

frictional forces: $\mathfrak{M}_{\mathrm{visc}} = -\mathfrak{M}$; the balance comes in a narrow transition layer where $\Lambda \neq 0$.

Conclusion.—We have shown that the axial ferrofluid pipe flow in a constant axial magnetic field becomes unstable via spontaneous symmetry breaking. Such an instability—like the Rosensweig free surface instability or the labyrinthine instability in thin ferrofluid layers—has no classical analogy. The origin of the concentric, two-phase swirling flow is due to a specific dependence of the magnetoviscosity on the shear rate; this dependence is provided by the competition between magnetic and viscous torques acting upon magnetic particles.

Our estimates [34] show that the swirling instability may be detected in available ferrofluids in magnetic fields about 100 Oe and Reynolds numbers of some tens.

[1] A. H. Shapiro, Nature (London) **196**, 1080 (1962).

[2] L. M. Trefethen, R. W. Bilger, P. T. Fink, R. E. Luxon, and R. I. Tanner, Nature (London) **207**, 1084 (1965).

[3] M. Kawakubo, Y. Tsuchiya, M. Sugaya, and K. Matsumura, Phys. Lett. A **68**, 65 (1978).

[4] R. Fernandez-Feria and E. Sanmiguel-Rojas, Phys. Fluids **12**, 3082 (2000).

[5] J. Mizushima, K. Abe, and N. Yokoyama, Phys. Rev. E **90**, 041002(R) (2014), see inset of Fig. 3.

[6] G. Quincke, Ann. Phys. Chem. **295**, 417 (1896).

[7] Recently, the Quincke effect was experimentally confirmed by L. Lobry and E. Lemaire, J. Electrost. **47**, 61 (1999).

[8] T. B. Jones, IEEE Trans. Ind. Appl. **IA-20**, 845 (1984).

[9] A. Cebers, Phys. Rev. Lett. **92**, 034501 (2004).

[10] G. Taylor, Proc. R. Soc. A **280**, 383 (1964).

[11] J. Fernandez de la Mora, J. Fluid Mech. **243**, 561 (1992).

[12] V. Shtern and A. Barrero, J. Fluid Mech. **300**, 169 (1995).

[13] M. A. Herrada and A. Barrero, Phys. Rev. E **66**, 036311 (2002).

[14] J. P. McTague, J. Chem. Phys. **51**, 133 (1969).

[15] R. E. Rosensweig, R. Kaiser, and G. Miskolczy, J. Colloid Interface Sci. **29**, 680 (1969).

[16] S. Kamiyama and A. Satoh, J. Magn. Magn. Mater. **85**, 121 (1990).

[17] J.-C. Bacri, R. Perzynski, M. I. Shliomis, and G. I. Burde, Phys. Rev. Lett. **75**, 2128 (1995).

[18] A. Zeuner, R. Richter, and I. Rehberg, Phys. Rev. E **58**, 6287 (1998); J. Magn. Magn. Mater. **201**, 321 (1999).

[19] R. Patel, R. V. Upadhyay, and R. V. Mehta, J. Colloid Interface Sci. **263**, 661 (2003).

[20] K. R. Schumacher, I. Sellien, G. S. Knoke, T. Cader, and B. A. Finlayson, Phys. Rev. E **67**, 026308 (2003).

[21] M. I. Shliomis, Sov. Phys. JETP **34**, 1291 (1972); Sov. Phys. Usp. **17**, 153 (1974).

[22] A. Zeuner, R. Richter, and I. Rehberg, J. Magn. Magn. Mater. **201**, 191 (1999).

[23] B. U. Felderhof, Phys. Rev. E **62**, 3848 (2000); **64**, 021508 (2001).

[24] A. P. Krekhov, M. I. Shliomis, and S. Kamiyama, Phys. Fluids **17**, 033105 (2005).

[25] H. C. Weng, C. L. Chen, and C. K. Chen, Phys. Rev. E **78**, 056305 (2008).

[26] S. Odenbach, *Magnetoviscous Effects in Ferrofluids*, Lecture Notes in Physics Vol. 71 (Springer, Heidelberg, 2002).

[27] M. I. Shliomis, T. P. Lyubimova, and D. V. Lyubimov, Chem. Eng. Commun. **67**, 275 (1988).

[28] S. Odenbach and H. Störk, J. Magn. Magn. Mater. **183**, 188 (1998).

[29] K. Morozov, M. Shliomis, and M. Zahn, Phys. Rev. E **73**, 066312 (2006).

[30] M. A. Martsenyuk, Y. L. Raikher, and M. I. Shliomis, Sov. Phys. JETP **38**, 413 (1974).[Zh. Eksp. Teor. Fiz. **65**, 834 (1973)].

[31] A. F. Pshenichnikov and V. V. Mekhonoshin, J. Magn. Magn. Mater. **213**, 357 (2000).

[32] In this case one can apply a mean-field model developed by P. Ilg and S. Hess, Z. Naturforsch. **58a**, 589 (2003); and tested in simulations by P. Ilg, M. Kröger, and S. Hess, Phys. Rev. E **71**, 031205 (2005); **71**, 051201 (2005).

[33] A. O. Ivanov, S. S. Kantorovich, E. N. Reznikov, C. Holm, A. F. Pshenichnikov, A. V. Lebedev, A. Chremos, and P. J. Camp, Phys. Rev. E **75**, 061405 (2007).

[34] See Supplemental Material at http://link.aps.org/supplemental/10.1103/PhysRevLett.118.114503 for details of calculations, which includes Ref. [35].

[35] M. I. Shliomis, in *Ferrofluids. Magnetically Controllable Fluids and Their Applications*, Lecture Notes in Physics, edited by S. Odenbach (Springer, Heidelberg, 2002), Vol. 594, p. 85.

[36] Radial component of Eq. (1) determines the radial pressure gradient, see the Supplemental Material [34].

[37] The linear stability of two-phase pipe flow of two miscible fluids with such and opposite viscosity stratification was studied by B. Selvam, S. Merk, R. Govindarajan, and E. Meiburg, J. Fluid Mech. **592**, 23 (2007).